

Article

Rapid Carbonation for Calcite from a Solid-Liquid-Gas System with an Imidazolium-Based Ionic Liquid

Abdul-Rauf Ibrahim [†], Jean Bosco Vuningoma [†], Yan Huang, Hongtao Wang and Jun Li ^{*}

Department of Chemical and Biochemical Engineering, College of Chemistry and Chemical Engineering, National Engineering Laboratory for Green Chemical Productions of Alcohols, Ethers and Esters, Xiamen University, Xiamen 361005, China; E-Mails: ghrauf@gmail.com (A.-R.I.); v29johannes@gmail.com (J.B.V.); yanh1236@gmail.com (Y.H.); wanght@xmu.edu.cn (H.W.)

[†] These authors contributed equally to this work.

^{*} Author to whom correspondence should be addressed; E-Mail: junnyxm@xmu.edu.cn; Tel./Fax: +86-592-218-3055.

Received: 8 May 2014; in revised form: 4 June 2014 / Accepted: 10 June 2014 /

Published: 25 June 2014

Abstract: Aqueous carbonation of $\text{Ca}(\text{OH})_2$ is a complex process that produces calcite with scalenohedral calcite phases and characterized by inadequate carbonate species for effective carbonation due to the poor dissolution of CO_2 in water. Consequently, we report a solid-liquid-gas carbonation system with an ionic liquid (IL), 1-butyl-3-methylimidazolium bromide, in view of enhancing the reaction of CO_2 with $\text{Ca}(\text{OH})_2$. The use of the IL increased the solubility of CO_2 in the aqueous environment and enhanced the transport of the reactive species (Ca^{2+} and CO_3^{2-}) and products. The presence of the IL also avoided the formation of the CaCO_3 protective and passivation layer and ensured high carbonation yields, as well as the production of stoichiometric rhombohedral calcite phases in a short time.

Keywords: calcite; carbon dioxide; carbonation; solid-liquid-gas; ionic liquid

1. Introduction

Calcium carbonate (CaCO_3) is an inorganic chemical that occurs in different crystalline polymorphs at ambient pressure. These are anhydrous phases of vaterite, calcite and aragonite and hydrated phases

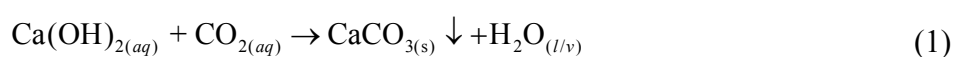
of monohydrocalcite and hexahydrocalcite (ikaite) [1]. Anhydrous CaCO_3 is generally classified as rhombic calcite, needle-like aragonite or spherical vaterite, among which calcite is the most stable phase under normal atmospheric conditions [2]. The formation of any of the polymorphs is strictly guided by the temperature, supersaturation and pH of reaction solution [3]. However, chameleonic phase transformation was found between calcite, aragonite and vaterite, normal to abnormal and *vice versa*, in a CO_2 expanded ethanol-water solution system applied for the solid-liquid-gas carbonation (SLGC) of $\text{Ca}(\text{OH})_2$ [4]. CaCO_3 is used for several industrial applications and by living organisms for bone development [5]. For instance, it is used as an extender and to meliorate stability and exposure to resistance in paints [6,7]. As such, global consumption and demand for CaCO_3 continues to increase [8,9]. Industrially, calcite is usually produced by the SLGC route, where CO_2 is bubbled through a $\text{Ca}(\text{OH})_2$ slurry or slake lime [10–13]. Although the mechanism for the precipitation of CaCO_3 from SLGC is debated, many investigators have shown that the absorption of CO_2 is the rate determining step in the SLGC with a $\text{Ca}(\text{OH})_2$ suspension [10,11]. Current synthesis procedures are slow, energy intensive and less efficient, leading to low conversion yields. Several methods for synthesizing CaCO_3 effectively and with various properties using additives and surfactants [14,15], block copolymers [16,17] and acids [18,19] have been explored.

The excellent role of ionic liquids (ILs) as reaction media and catalysts is common knowledge, among which, imidazolium-based ILs are the most researched group. Studies have shown that the solubility of CO_2 in this group of ILs increases with increased pressure [20,21]. For example, Sudha and Khanna [22] in a molecular modeling of the solubility of CO_2 in several ILs reported the solubility of CO_2 in 1-butyl-3-methylimidazolium bromide, Bmim[Br], to be a 0.31 molar fraction. Once the absorption of CO_2 is a rate determining step in the SLGC with the $\text{Ca}(\text{OH})_2$ suspension and CO_2 is very soluble in ILs, coupling an SLGC system with an IL will enhance the absorption of CO_2 and lead to higher conversion yields.

Previously, we conducted systematic research on a solid-gas carbonation (SGC) involving a dry $\text{Ca}(\text{OH})_2$ system with a solid ionic liquid (SIL) and high-pressure/supercritical CO_2 and achieved the complete conversion of $\text{Ca}(\text{OH})_2$ to CaCO_3 in 5 min [23,24]. The SIL served as the catalyst carrier and facilitated the effective dissolution of CO_2 , leading to the syntheses of stoichiometric rhombohedral calcite phases [23,24]. In the current study, we report an SLGC involving a $\text{Ca}(\text{OH})_2$ slurry system using an imidazolium-based IL in view of enhancing carbonation efficiency. The study searches for rapid carbonation for the production of nano- CaCO_3 and the capture of CO_2 , since CO_2 capture is an important industrial application [23]. The IL was used in the current work as a reaction media to increase the solubility of CO_2 and to enhance the kinetics of the reaction in the liquid phase. Note that the IL is very miscible with water and can easily be recovered.

2. Results and Discussion

Precipitation of CaCO_3 from aqueous carbonation of $\text{Ca}(\text{OH})_2$ is an exothermic and complex process with an overall reaction equation as [5,7]:

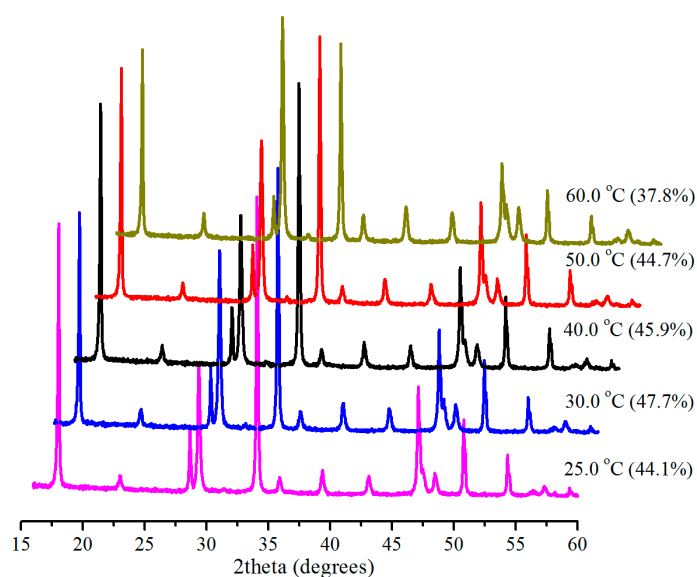


Traditionally, SLGC produces calcite with a scalenohedral lattice $\{2\ 1\ -1\}$ [25,26] and is characterized by excess calcium species (Ca^{2+}) as a result of the limited solubility of CO_2 in water [27–29], leading to inadequate carbonate species (CO_3^{2-}) necessary for producing the stoichiometric rhombohedral phase [24,27]. Thus, any process that enhances the solubility of CO_2 and the dissolution of $\text{Ca}(\text{OH})_2$ can positively affect the reaction rate and result in higher conversion yields. Therefore, increasing the solubility of CO_2 using an IL to facilitate the effective dissolution of $\text{Ca}(\text{OH})_2$ will not only enhance carbonation yields, but also facilitate and produce the stoichiometric rhombohedral calcite phase [24,27].

2.1. Effect of Temperature

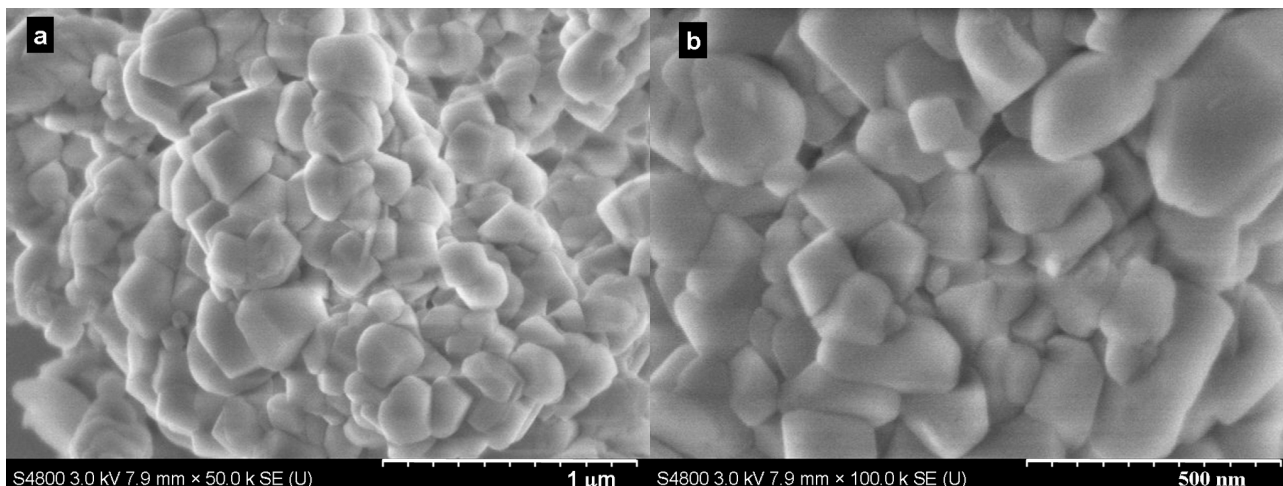
The effect of temperature on SLGC is well-known [7], and lower temperature is commonly adopted to increase the solubility of CO_2 in water. We investigated the effect of temperature (25.0, 30.0, 40.0, 50.0 and 60.0 °C) at atmospheric pressure (0.1 MPa) in 5 min with 0.5 g Bmim[Br]/5.0 g $\text{Ca}(\text{OH})_2$ and 10 mL water. X-ray diffractometry (XRD) patterns of the produced samples and the corresponding conversions of $\text{Ca}(\text{OH})_2$ at the different temperatures are shown in Figure 1. As can be seen, the conversion increased from 44.1% at 25.0 °C to only 45.9% at 40.0 °C and then decreased slightly to 37.8% at 60.0 °C, revealing that temperature did not have an obvious effect on the system and that the IL took effect. The highest conversion (47.7%) for the 0.1 MPa reactions, although not complete, is about the best value reported for identical systems with shorter reaction times in the literature, indicating the availability of the IL.

Figure 1. XRD (X-ray diffractometry) patterns and corresponding conversions (in brackets) for samples produced with 1-butyl-3-methylimidazolium bromide (Bmim[Br]) at various temperatures with 0.1 MPa in 5 min.



The samples were also characterized by scanning electron microscope (SEM) to investigate their morphology (typically shown in Figure 2). The SEM images revealed that irregular rhombohedral calcite (ICCD-PDF-2: 01-086-2334) particles were produced at the conditions investigated. Additionally, there was no unique and distinct difference between the particles produced.

Figure 2. SEM (scanning electron microscope) images of samples produced at (a) 40.0 °C and (b) 60.0 °C with 0.1 MPa in 5 min.



2.2. Effect of Pressure

Figure 3 shows the effect of pressure on the conversion at 30.0 °C in 5 min with 0.5 g Bmim[Br]/5.0 g Ca(OH)₂ and 10 mL water. At 0.1 MPa, there was incomplete conversion, because a 47.7% conversion was realized. This was evidenced by the presence of the characteristic peaks for both the starting material (at 18.0° and 34.2°) and the product (at 29.4°). A similar phenomenon was witnessed for the reaction at 1.0 MPa, resulting in a 64.7% conversion. However, at 5.0 MPa, the major peaks of the starting material almost disappeared, leading to pronounced major peaks of the product and substantial conversion (99.1%). Yet, a further increase of the pressure reduced the conversion slightly (Figure 3). The presence of the Bmim[Br] increased the conversions at 0.1 and 1.0 MPa (Figure 3). The quantity of dissolved CO₂ needed to produce CO₃²⁻ species for carbonation is restricted by the low solubility of CO₂ in water at low pressures [5], but the Bmim[Br] enhanced the availability of the CO₃²⁻ species, due to the high solubility of CO₂ in the IL [22] and led to the high conversion yields.

Figure 3. XRD patterns and corresponding conversions (in brackets) for samples produced with Bmim[Br] at various pressures at 30.0 °C in 5 min.

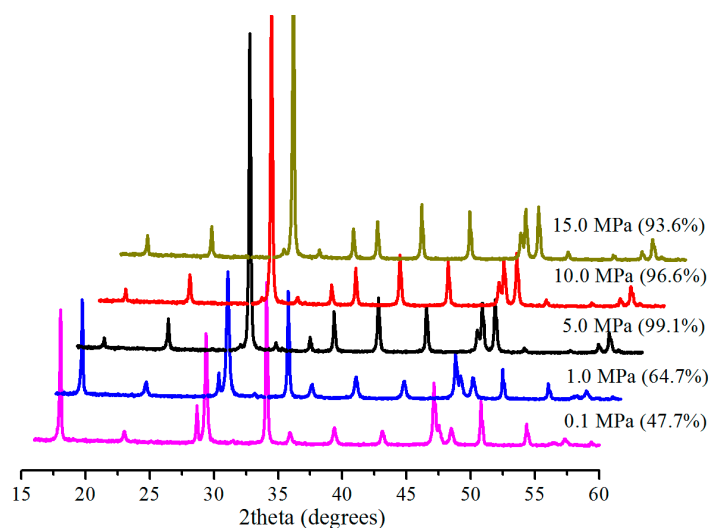
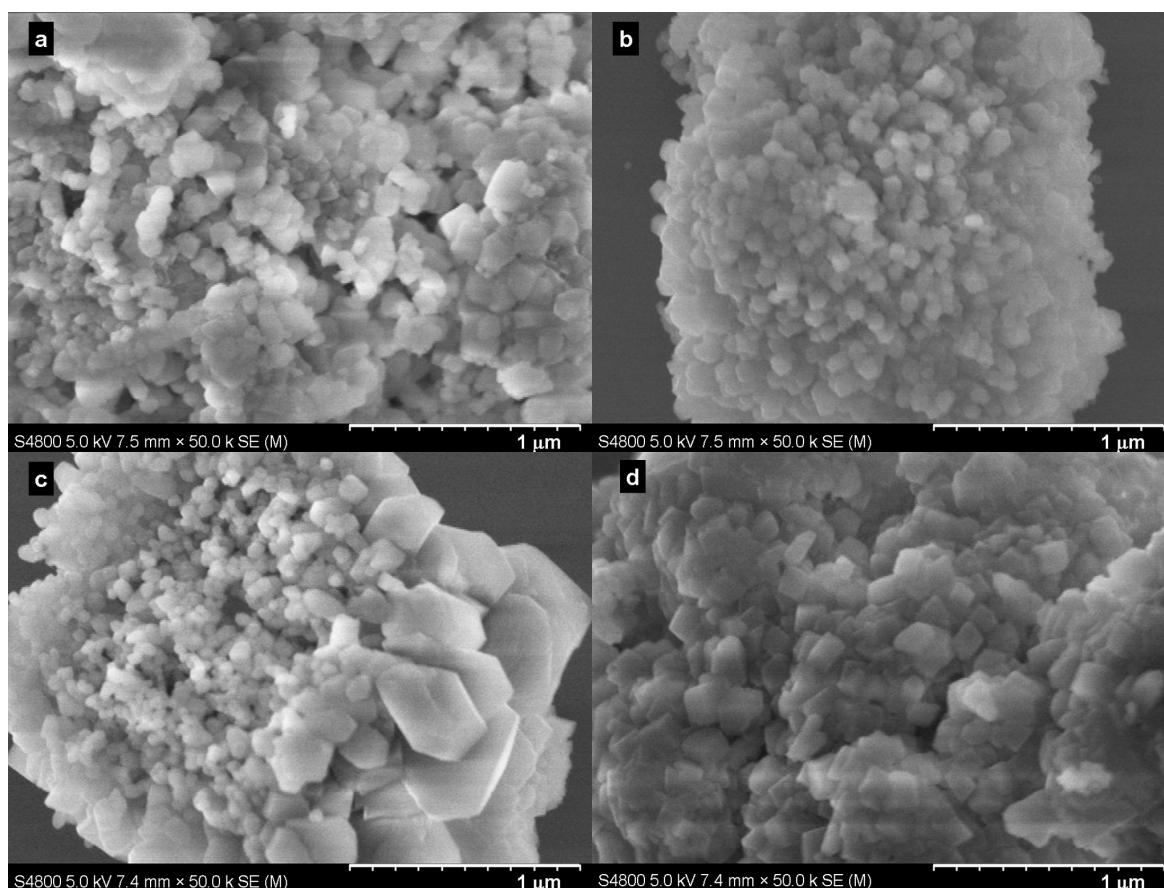


Figure 4 shows typical SEM images of the samples produced at various pressures. The images confirmed the rhombohedral, but agglomerated, nature of the particles produced. A comparison of the particles produced at 5.0 MPa with Bmim[Br] (Figure 4c) and without Bmim[Br] (Figure 4d) revealed that the former sample consisted of the majority of less agglomerated and irregular, but smaller (≈ 60 nm) particles with a minority of bigger (≈ 300 nm) rhombohedral ones, while the latter sample had almost uniform, but highly agglomerated and bigger (≈ 100 nm) rhombohedral particles. Note that the conversion without the IL at 5.0 MPa and 30.0 °C in 5 min was 52.7%.

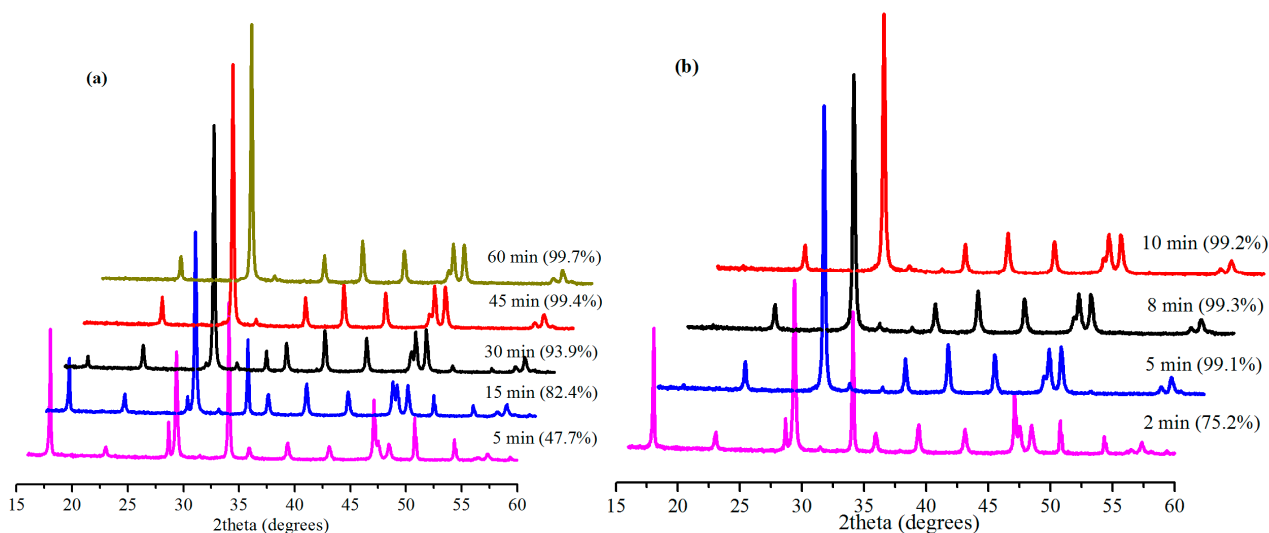
Figure 4. SEM images of samples produced with Bmim[Br] at (a) 0.1 MPa; (b) 1.0 MPa; (c) 5.0 MPa and without Bmim[Br] at (d) 5.0 MPa in 5 min at 30.0 °C.



2.3. Effect of Reaction Time

The extent of carbonation reaction is a function of time; hence, the effect of reaction time on the rate of conversion was investigated. Figure 5 shows the effect of reaction time on the conversion of $\text{Ca}(\text{OH})_2$ with 0.5 g Bmim[Br]/5.0 g $\text{Ca}(\text{OH})_2$ and 10 mL water at 30.0 °C for 0.1 and 5.0 MPa. At 0.1 MPa, the slow reaction led to low conversion (26.3%) after 5 min without Bmim[Br]. The conversion increased to 34.6% in 30 min and 65.3% in 60 min without the IL. However, it was 47.7% in 5 min when the IL was introduced, but increased to 93.9% in 30 min and then 99.7% after 60 min. Obviously, the effect of the IL on the conversion at this low pressure was significant especially, within 30 min. The conversion increased from 34.6% in 30 min without the IL to 93.9% ($\approx 59.3\%$ increment) when the IL was added.

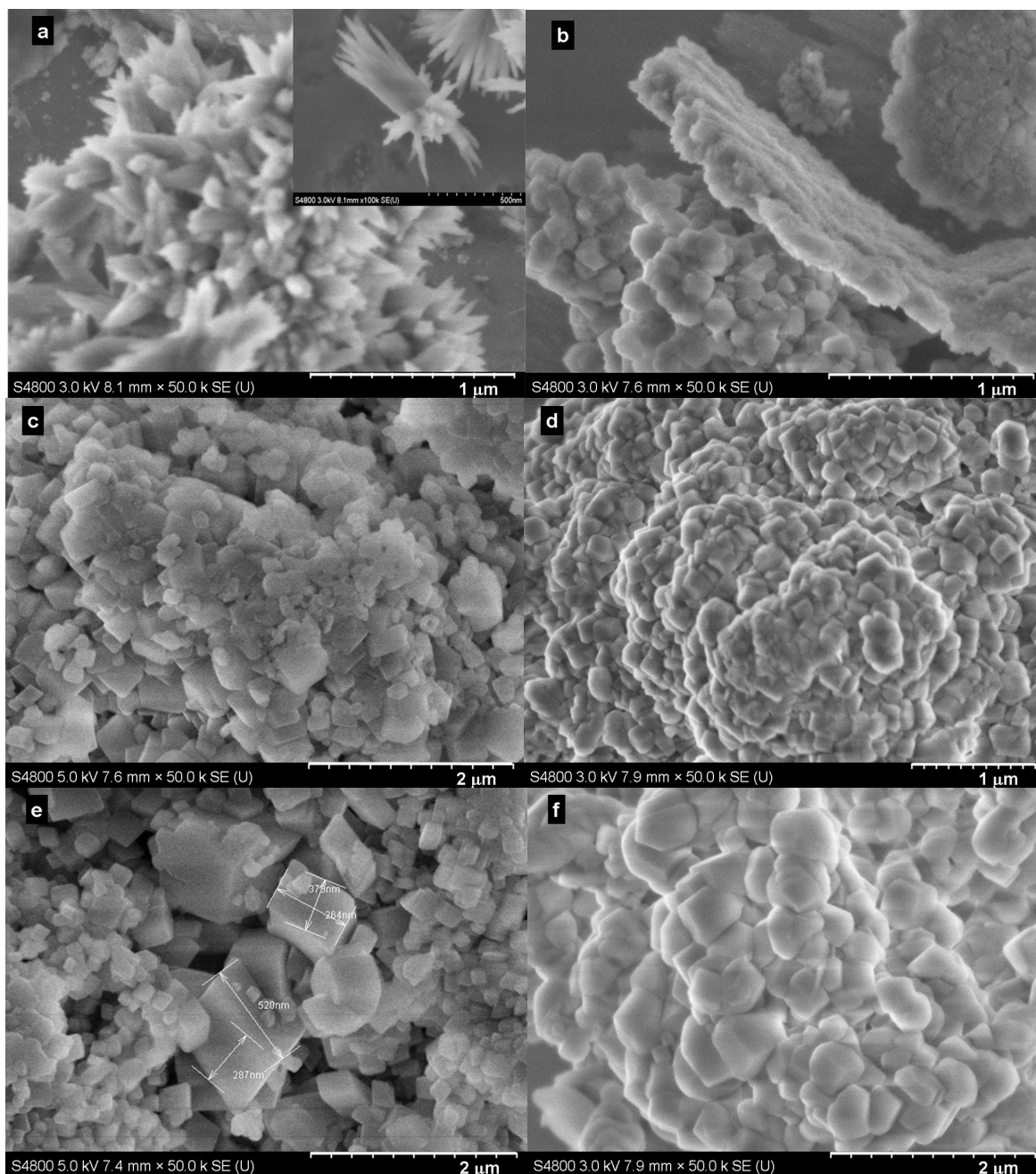
Figure 5. XRD patterns and corresponding conversions (in brackets) for samples produced with Bmim[Br] with different reaction times at (a) 0.1 MPa and (b) 5.0 MPa.



Among other parameters, increasing the working pressure of CO₂ increases its solubility and, by extension, the availability of CO₃²⁻ species in the SLGC for better yield [5]. In this regard, several experiments were carried out at 5.0 MPa with the Bmim[Br] to investigate the effect of time. For these cases, the reactions were very fast (almost complete conversions) within 5 min. Even so, when the reaction was monitored over a very short time (2 min), the positive influence of the IL was evident. The reaction resulted in a 75.2% conversion demonstrating the ability of the IL to facilitate faster reaction in the initial stages of the carbonation at medium pressure (5.0 MPa). Furthermore, a 47.7% conversion was obtained at 0.1 MPa in 5 min, whereas the conversion was 99.3% at 5.0 MPa, confirming the fast nature of the reaction in the presence of the IL at the medium pressure.

Representative SEM images for the samples produced at selected times are shown in Figure 6. Generally, and as expected, the samples produced with the Bmim[Br] exhibited well-defined particles (Figure 6a,c,e) compared to those produced without the IL (Figure 6b,d,f). Additionally, the effect of time on morphology was clearly visible. For instance, whereas the sample produced with the IL in 5 min consisted of a mixture of flower-like calcite (≈50 nm) and bundle-like hexagonal (inset) Ca(OH)₂ particles (≈50 × 900 nm; Figure 6a), those produced in 30 min showed a perfect mixture of smaller (≈50 nm) and larger (≈400 nm) rhombohedral calcites (Figure 6c). However, the SEM images (Figure 6) indicated the obvious increase of particle size following the reaction time. Note that Figures 4a and 6a are different images of the same sample; Figure 6a was deliberately taken to show both Ca(OH)₂ and calcite particles, whereas Figure 4a showed only calcite particles.

Figure 6. SEM images of the samples produced at 30.0 °C and 0.1 MPa. (a) with Bmim[Br] and (b) without Bmim[Br] in 5 min; (c) with Bmim[Br] and (d) without Bmim[Br] in 30 min; (e) with Bmim[Br] and (f) without Bmim[Br] in 60 min.

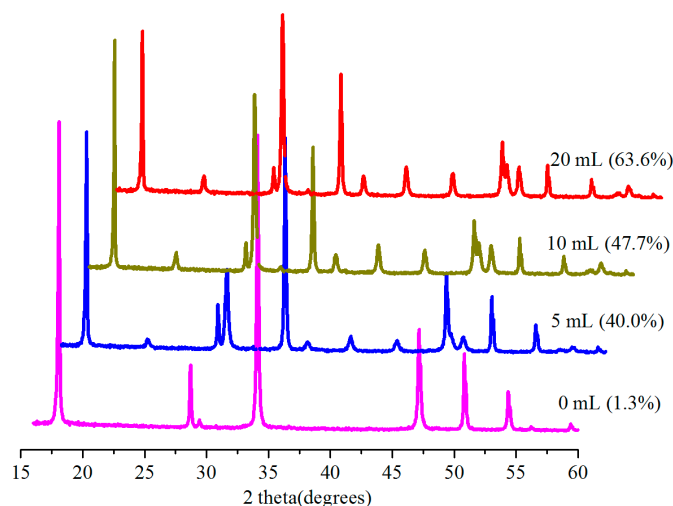


2.4. Effect of Amount of Water

Water is very vital for carbonation reactions, and the role of water has been reported accordingly [5,23]. The influence of the amount of water on conversion was thus investigated at 0.1 MPa and 30.0 °C in 5 min with 0.5 g Bmim[Br]/5.0 g Ca(OH)₂. For the zero-milliliter (0 mL) water, the IL was dried under vacuum for 36 h to remove traces of adsorbed water, and no additional water was added into the reactor during the reaction; so it was a dry carbonation (SGC) system [23]. The conversion results are shown in Figure 7, revealing increased conversion with an increasing amount of water. A conversion of 40.0% was obtained using 5.0 mL as opposed to 1.3% for the reaction without water (0 mL), but the

conversion increased to 63.6% with 20.0 mL of water. Note that these were slurry systems and, as such, suspensions; hence the mentioning of the presence of water instead of concentrations or solutions.

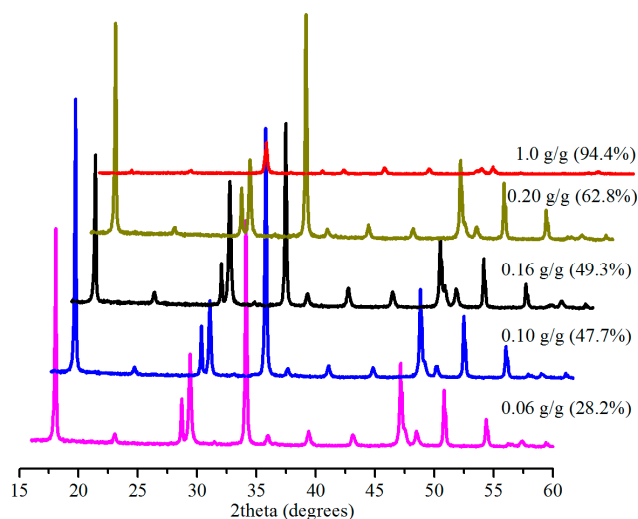
Figure 7. XRD patterns and corresponding conversions (in brackets) for samples produced with the Bmim[Br] and various amounts of water at 0.1 MPa and 30.0 °C in 5 min.



2.5. Effect of Amount of Bmim[Br]

The presence of Bmim[Br] was shown to have a significant effect on the conversion at the low (0.1 MPa) and medium (5.0 MPa) pressures in 5 min (see Sections 2.2 and 2.3). Therefore, we investigated the effect of the mass ratio of the IL to $\text{Ca}(\text{OH})_2$ on the conversion at 0.1 MPa within 5 min at 30.0 °C. Figure 8 shows the conversion results of the samples produced, revealing increased conversion from 28.2% at 0.06 g IL/g $\text{Ca}(\text{OH})_2$ to 94.4% at 1.0 g IL/g $\text{Ca}(\text{OH})_2$. We are mindful of the comparatively expensive nature of ILs. However, about a 30% conversion of $\text{Ca}(\text{OH})_2$ at 0.1 MPa with just 6% (0.06 g IL/1 g $\text{Ca}(\text{OH})_2$) of the IL and a 99.1% conversion at 5.0 MPa with 10% (0.5 g IL/5 g $\text{Ca}(\text{OH})_2$) of the IL in 5 min, perhaps, justify the use of the IL in terms of cost.

Figure 8. XRD patterns and corresponding conversions (in brackets) for samples produced with 10 mL water and various amounts of Bmim[Br] in 5 min.



2.6. Significance of Bmim[Br] and the Mechanism

Enhanced dissolution of CO₂ is among the key parameters that control carbonation reactions, and for SLGC, enhancing the solubility of CO₂ in water is particularly important. As such, the use of the IL was expected to enhance the production of the CO₃²⁻ from the effective dissolution of CO₂ in the IL [22] and affect conversion yields. The influence of the IL on conversion was evident at lower pressure. For example, with 0.1 MPa at 30.0 °C in 5 min, the reaction without the IL gave a conversion of 26.3% against about 50% with the IL (Figure 8). Furthermore, the effect of the IL on the particle size and degree of agglomeration at the medium pressure (5.0 MPa) was noticeable. The sample produced with the IL was a mixture of smaller (≈60 nm) and bigger (≈300 nm) rhombohedral particles with less agglomeration (Figure 4c), whereas the particles synthesized without the IL were bigger rhombohedrals (≈100 nm) with more agglomeration (Figure 4f). The IL also had a positive influence on the conversion (99.1%) in 5 min at the medium pressure, however; its availability was prominent when the reaction was monitored for 2 min (75.0% conversion), indicating that it induced a faster reaction within the initial stage of the carbonation. On the other hand, reaction with 0.10 g IL/g Ca(OH)₂ in 5 min resulted in a conversion of 47.7%. A decreased amount of the IL (0.06 g IL/g Ca(OH)₂ in 5 min), as expected, only worsened the conversion yield (28.2%), while an increased amount of the IL (1.0 g IL/g Ca(OH)₂ in 5 min) gave a conversion (94.4%) greater than 90.0%. Considering the cost implications of ILs, 1.0 g IL/g Ca(OH)₂ in 5 min for a 94.4% conversion may not be industrially prudent, although the IL may be recovered. Therefore, we suggest an optimum of 0.10 g IL/g Ca(OH)₂ (10% IL), but in 30 min, because a conversion of 93.9% was obtained in this case, even though a 99.7% conversion was realized in 60 min.

The mechanism of the current SLGC system with Bmim[Br] is therefore similar to that of the SGC system with the solid ionic liquid previously reported [23,24]. Briefly, the Bmim[Br] absorbs water and CO₂ to initiate the reaction by forming hydrated layers. These layers promote the dissolution of Ca(OH)₂ to produce Ca²⁺ species and the conversion of CO₂ to CO₃²⁻ species. Because of the relatively high solubility of CO₂ in Bmim[Br], there is enough CO₃²⁻ avoiding the formation of the usual protective and passivation CaCO₃ layer, and this led to the formation of stoichiometric rhombohedral calcite particles.

2.7. Brunner-Emmet-Teller (BET) Surface Area and Thermogravimetric Analysis (TGA)

BET analysis was done to study the specific surface area and pore structure of the sample synthesized with the IL at 5.0 MPa and 30 °C in 5 min, since this gave almost complete conversion (99.1%). A surface area of 13.0 m²/g was obtained. This result is comparable with values reported for SLGCs with similar conditions [4,30], but better than values reported for some SGCs [27]. The highest surface area for a similar system, but with a rotating disc reactor unit at ambient conditions, was reported to be between 20.4 and 23.3 m²/g; however, the products were filtered through a 0.1-μm membrane [31].

The thermal stability of the samples produced at the lower and medium pressures was studied with a thermogravimetric analyzer. As shown in Figure 9, the total weight loss was 47.7% for the sample produced at 5.0 MPa, whilst a total weight loss of 34.6% was noticed for the sample produced at 0.1 MPa. The TGA results enabled the validation of the Rietveld whole pattern refinement of the XRD

analysis (see Table 1). For this case, the weight loss due to the release of physically adsorbed water, the release of water from $\text{Ca}(\text{OH})_2$ and the release of CO_2 from CaCO_3 as a result of thermal decomposition were recorded, and the weight percent of CaCO_3 in the sample was calculated with Equation (2).

$$\text{CaCO}_3 [\text{wt } \%] = \frac{W_L}{W_T} \times \frac{M_{\text{CaCO}_3}}{n \times M_{\text{CO}_2}} \times 100 \quad (2)$$

where W_T denotes the total weight of the sample (g), W_L denotes the weight loss (g), n denotes the number of moles of CO_2 eliminated and M denotes molecular weight (g/mol).

Figure 9. Thermogravimetric curves for the CaCO_3 produced: (a) 5.0 MPa and (b) 0.1 MPa in 5 min at 30.0 °C.

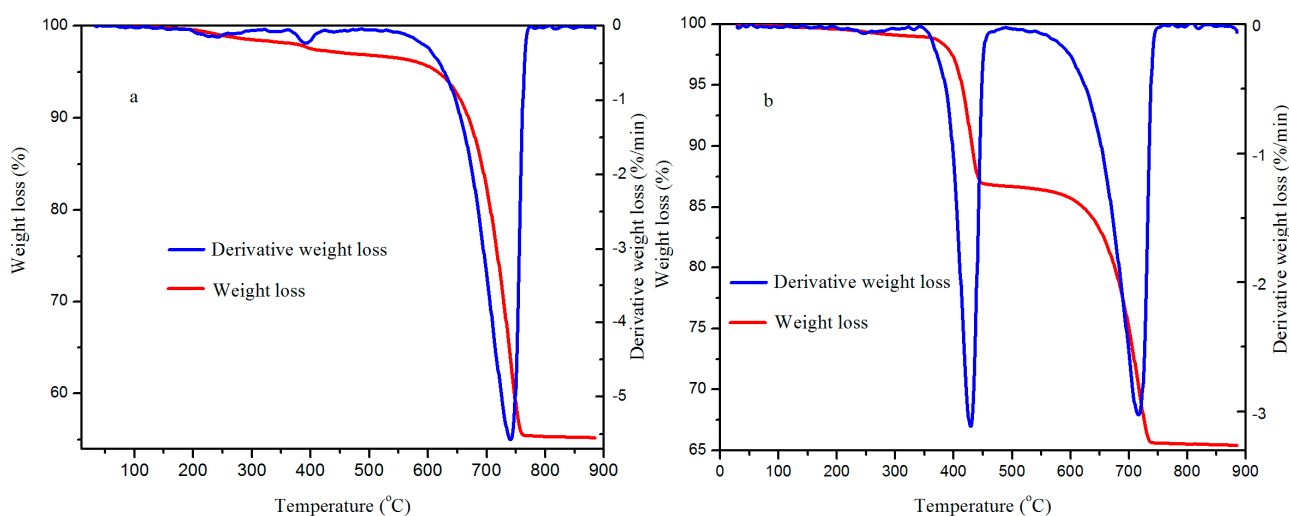


Table 1. Validation of XRD Rietveld refinements by TGA.

Sample	Rietveld (wt %)	TGA (wt %)	Difference (wt %)
5.0 MPa	99.1	96.2	2.9
0.1 MPa	47.7	49.7	2.0

The endothermic peak at about 740.6 °C for the sample produced at 5.0 MPa led to about 96.2% (mass) CaCO_3 . Similarly, the endothermic peaks at about 428.6 °C attributed to decomposition of $\text{Ca}(\text{OH})_2$ and at about 716.6 °C assigned to the decomposition of CaCO_3 for the sample produced at 0.1 MPa correspond to about 49.7% CaCO_3 . These percentage values are in agreement with the results from the Rietveld refinements for the XRD patterns (Table 1).

3. Experimental Section

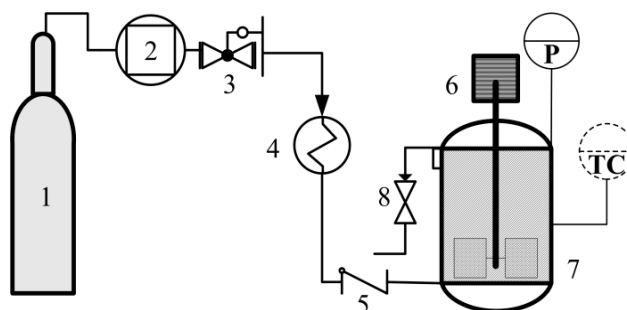
3.1. Materials

Analytical grade $\text{Ca}(\text{OH})_2$ with 95% purity was purchased from Sinopharm Chemical and Reagents Co., Ltd, Shanghai, China. Carbon dioxide (99.99% purity) was sourced from Linde Gas, Xiamen Corporation Ltd., Xiamen, China, and 1-butyl-3-methylimidazolium bromide, Bmim[Br] with 99% purity was purchased from Shanghai Cheng Jie Chemical Co., Ltd., Shanghai, China.

3.2. Procedure

The setup for the process is shown in Figure 10, consisting of a CO₂ cylinder (G447-400, Beijing HuiZhi M&E Facilities Co., Ltd., Beijing, China), a self-modified back pressure regulator (± 0.1 MPa), a preheater, a check valve and a high pressure reactor (100 mL) with a maximum internal working pressure of 30 MPa, a temperature of 300 °C and outlet and inlet valves arranged, such that CO₂ could be bubbled straight into the bulk of the slurry and discharged immediately after the reaction. The reactor is equipped with a mechanical stirrer (about 500 rpm), thermocouple, a pressure meter and a temperature controller (± 0.1 °C).

Figure 10. Illustration of the experimental setup: 1, CO₂ cylinder; 2, compressor; 3, back pressure regulator; 4, preheater; 5, check valve; 6, mechanical stirrer; 7, reactor; 8, outlet valve; TC, temperature controller; P, pressure indicator.



Typically, an amount of distilled water (mL) was added to 5.0 g of Ca(OH)₂ to produce a slurry. To this, Bmim[Br] of mass ratios of 0.5 g/5 g Ca(OH)₂ was loaded into the reaction vessel and heated under stirring (500 rpm) until thermal equilibrium (°C). CO₂ was fed into the vessel, brought to the desired pressure (MPa) and reacted for a set time (min). CO₂ was deliberately released after the reaction; the product was collected, washed to recover the ionic liquid and dried in an oven (Jinhong, DZF-6020, Shanghai, China) at 100 °C for 12 h.

3.3. Characterization

The phase purity and quantity of the samples were analyzed with X-ray diffractometry (XRD), and the crystallite size was determined using Jade 5.0 from XRD patterns. Measurements of the XRD were carried out using X'Pert Pro (PANalytical B.V, Ea Almelo, The Netherlands) with a Cu anode operated at 40 kV, 30 mA and a wavelength (λ) of 1.540598 Å. A continuous scan from 16° to 60° with a 2-theta step scan of 0.016711° and a step length of 10 s was employed. Calcite has a characteristic major peak at 29.41° corresponding to the {1 0 4} reflection plane, while Ca(OH)₂ has a major peak at 34.11°, matching the {0 0 1} reflection plane, followed by the peak at 18.08° [24]. In our case, however, the Ca(OH)₂ peak at 18.08° was the highest. Phase analysis and quantification was achieved by Rietveld whole pattern refinements using X'Pert HighScore plus (2.0) and the ICDD-PDF-2 database [24]. Specific surface area and pore size were determined by BET (Micrometric TRISTAR-3000, Micromeritics Instrument Corporation, Norcross, GA, USA), and isotherms were obtained by performing isothermal physical sorption with N₂ gas at 77.3 K. SEM (S4800, Hitachi, Tokyo, Japan) was employed to study the morphology of the samples by dispersing samples

ultrasonically in absolute ethanol for 30 min and depositing on a silicon wafer. Thermal stability was studied by thermogravimetric analysis (NETZSCH TG 209 F1, Selb, Germany) under N₂ from 30 to 900 °C with a heating rate of 10 °C/min.

4. Conclusions

We investigated the effect of several variables on an SLG carbonation system using Ca(OH)₂ slurry with an imidazolium-based IL, Bmim[Br]. Based on the results, we conclude that: (1) the use of the IL positively influenced the carbonation reaction at relatively low pressure (0.1 MPa), such that with 1 g IL/1 g Ca(OH)₂, a conversion higher than 94.4% was achieved within 5 min; (2) the optimum condition (0.10 g IL/1 g Ca(OH)₂ in 30 min) at the lower pressure gave a conversion of 93.9%; (3) medium pressure (5.0 MPa) led to almost complete conversion (99.6%) in 5 min; (4) 5.0 mL of water or more was necessary for the rapid conversion of 5.0 g Ca(OH)₂, yet the removal of water from the system gave very low conversion; (5) the samples exhibited rhombohedral calcite structures with a high specific surface area; and (6) the amount of CaCO₃ obtained from the Rietveld refinement of XRD patterns was very close to that obtained from TG analysis.

Acknowledgments

This work was supported by National Nature Science Foundation of China (NSFC) (No. 21276212) and Specialized Research Fund for the Doctoral Program of Higher Education (SRFDP) (No. 20100121110009).

Author Contributions

A.-R.I. and J.B.V. conducted the experiments, analyses and calculations. Y.H. participated in the experiments. J.L. and H.T.W. conceived of and designed the research.

Conflicts of Interest

The authors declare no conflict of interest.

References

1. Gomez-Villalba, L.S.; Lopez-Arce, P.; de Buergo, M.A.; Fort, R. Atomic defects and their relationship to aragonite-calcite transformation in portlandite nanocrystal carbonation. *Cryst. Growth Des.* **2012**, *12*, 4844–4852.
2. Knez, S.; Klinar, D.; Golob, J. Stabilization of PCC dispersions prepared directly in the mother-liquid after synthesis through the carbonation of (hydrated) lime. *Chem. Eng. Sci.* **2006**, *61*, 5867–5880.
3. Montes-Hernandez, G.; Daval, D.; Chiriach, R.; Renard, F. Growth of nanosized calcite through gas-solid carbonation of nanosized portlandite under anisobaric conditions. *Cryst. Growth Des.* **2010**, *10*, 4823–4830.

4. Ibrahim, A.R.; Zhang, X.L.; Hong, Y.Z.; Wang, H.T.; Li, J. Instantaneous solid-liquid-gas carbonation of Ca(OH)₂ and chameleonic phase transformation in CO₂-expanded solution. *Cryst. Growth Des.* **2014**, *14*, 2733–2741.
5. Domingo, C.; Loste, E.; Gomez-Morales, J.; Garcia-Carmona, J.; Fraile, J. Calcite precipitation by a high-pressure CO₂ carbonation route. *J. Supercrit. Fluids* **2006**, *36*, 202–215.
6. Ciullo, P.A. *Industrial Minerals and Their Uses: A Handbook and Formulary*; Noyes Publications: Westwood, NJ, USA, 1996; pp. 35–37.
7. Montes-Hernandez, G.; Renard, F.; Geoffroy, N.; Charlet, G.; Pironon, J. Calcite precipitation from CO₂-H₂O-Ca(OH)₂ slurry under high pressure of CO₂. *J. Cryst. Growth* **2007**, *308*, 228–236.
8. Harja, M.; Cimpeanu, C.; Bucur, R.D. The influence of hydrodynamic conditions on the synthesis of ultra-thin calcium carbonate. *J. Food Agric. Environ.* **2012**, *10*, 1191–1195.
9. Juvekar, V.A.; Sharma, M.M. Absorption of CO₂ in a suspension of lime. *Chem. Eng. Sci.* **1973**, *28*, 825–837.
10. Sada, E.; Kumazawa, H.; Lee, C.; Fujiwara, N. Gas-liquid mass transfer characteristics in a bubble column with suspended sparingly soluble fine particles. *Ind. Eng. Process Des. Dev.* **1985**, *24*, 255–261.
11. Xiang, L.; Xiang, Y.; Wen, Y.; Wei, F. Formation of CaCO₃ nanoparticles in the presence of terpeneol. *Mater. Lett.* **2004**, *58*, 959–965.
12. Yagi, H.; Iwazawa, A.; Sonobe, R.; Matsubara, T.; Hikita, H. Crystallization of calcium carbonate accompanying chemical absorption. *Ind. Eng. Chem. Fundam.* **1984**, *23*, 153–158.
13. Meldrum, F.C.; Hyde, S.T. Morphological influence of magnesium and organic additives on the precipitation of calcite. *J. Cryst. Growth* **2001**, *231*, 544–558.
14. Qi, L.; Li, J.; Ma, J. Biomimetic morphogenesis of calcium carbonate in mixed solutions of surfactants and double-hydrophilic block copolymers. *Adv. Mater.* **2002**, *14*, 300–303.
15. Colfen, H.; Qi, L. A systematic examination of the morphogenesis of calcium carbonate in the presence of a double-hydrophilic block copolymer. *Chem. A Eur. J.* **2001**, *7*, 106–116.
16. Rudloff, J.; Antonietti, M.; Colfen, H.; Pretula, J.; Kaluzynski, K.; Penczek, S. Double-hydrophilic block copolymers with monophosphate ester moieties as crystal growth modifiers of CaCO₃. *Macromol. Chem. Phys.* **2002**, *203*, 627–635.
17. Mann, S.; Heywood, B.R.; Rajam, S.; Birchall, J.D. Controlled crystallisation of CaCO₃ under stearic acid monolayers. *Nature* **1988**, *334*, 692–965.
18. Naka, K.; Huang, S.C.; Chujo, Y. Formation of stable vaterite with poly(acrylic acid) by the delayed addition method. *Langmuir* **2006**, *22*, 7760–7767.
19. Aki, S.N.V.K.; Mellein, B.R.; Saurer, E.M.; Brennecke, J.F. High-pressure phase behavior of carbon dioxide with imidazolium-based ionic liquids. *J. Phys. Chem. B* **2004**, *108*, 20355–20365.
20. Anthony, J.L.; Maginn, E.J.; Brennecke, J.F. Solution thermodynamics of imidazolium-based ionic liquids and water. *J. Phys. Chem. B* **2001**, *105*, 10942–10949.
21. Cadena, C.; Anthony, J.L.; Shah, J.K.; Morrow, T.I.; Brennecke, J.F.; Maginn, E.J. Why is CO₂ so soluble in imidazolium-based ionic liquids? *J. Am. Chem. Soc.* **2004**, *126*, 5300–5308.
22. Sudha, S.Y.; Khanna, A. Evaluation of CO₂-ionic liquid systems through molecular modeling. *World Acad. Sci. Eng. Technol.* **2009**, *57*, 539–542.

23. Ibrahim, A.-R.; Vuningoma, J.B.; Hu, X.H.; Gong, Y.; Dan, H.; Hong, Y.Z.; Wang, H.T.; Li, J. High-pressure gas-solid carbonation route coupled with a solid ionic liquid for rapid synthesis of rhombohedral calcite. *J. Supercrit. Fluids* **2012**, *72*, 78–83.
24. Ibrahim, A.-R.; Gong, Y.; Hu, X.H.; Hong, Y.Z.; Su, Y.Z.; Wang, H.T.; Li, J. Solid-gas carbonation coupled with solid ionic liquid for synthesis of CaCO₃: Performance, polymorphic control and self-catalytic kinetics. *Ind. Eng. Chem. Res.* **2013**, *52*, 9515–9524.
25. Lopez-Periago, A.M.; Pacciani, R.; Garcia-Gonzalez, C.; Vega, L.F.; Domingo, C. A breakthrough technique for the preparation of high-yield precipitated calcium carbonate. *J. Supercrit. Fluids* **2010**, *52*, 298–305.
26. Chen, P.C.; Tai, C.Y.; Lee, K.C. Morphology and growth rate of calcium carbonate crystals in a gas-liquid-solid reactive crystallizer. *Chem. Eng. Sci.* **1997**, *52*, 4171–4177.
27. Montes-Hernandez, G.; Pommerol, A.; Renard, F.; Beck, P.; Quirico, E.; Brissaud, O. *In situ* kinetic measurements of gas-solid carbonation of Ca(OH)₂ by using an infrared microscope coupled to a reaction cell. *Chem. Eng. J.* **2010**, *161*, 250–256.
28. Beruto, D.T.; Botter, R. Liquid-like H₂O adsorption layers to catalyse the Ca(OH)₂/CO₂ solid-gas reaction and to form a non-protective solid product layer at 20 °C. *J. Eur. Ceram. Soc.* **2000**, *20*, 497–503.
29. Dickinson, S.R.; Henderson, G.E.; McGrath, K.M. Controlling the kinetic *versus* thermodynamic crystallisation of calcium carbonate. *J. Cryst. Growth* **2002**, *244*, 369–378.
30. Lopez-Periago, A.M.; Pacciani, R.; Vega, L.F.; Domingo, C. Monitoring the effect of mineral precursor, fluid phase CO₂-H₂O composition, and stirring on CaCO₃ crystallization in a supercritical-ultrasound carbonation process. *Cryst. Growth Des.* **2011**, *11*, 5324–5332.
31. Kedra-Krolik, K.; Gierycz, P. Precipitation of nano-structured calcite in a controlled multiphase process. *J. Cryst. Growth* **2009**, *311*, 3674–3681.

© 2014 by the authors; licensee MDPI, Basel, Switzerland. This article is an open access article distributed under the terms and conditions of the Creative Commons Attribution license (<http://creativecommons.org/licenses/by/3.0/>).